



1 **Nitrogen deposition and climate drive plant nitrogen uptake while**
2 **soil factors drive nitrogen use efficiency in terrestrial ecosystems**

3

4 Helena Vallicrosa^{1,2,3}, Katrin Fleischer^{4,5}, Manuel Delgado-Baquerizo⁶, Marcos Fernández-Martínez⁷, Jakub
5 Černý⁸, Di Tian⁹, Angeliki Kourmouli^{10,11}, Carolina Mayoral^{11,12}, Diego Grados¹³, Mingzhen Lu^{14,15}, César
6 Terror¹

7

8 **1** Department of Civil and Environmental Engineering, Massachusetts Institute of Technology, Cambridge,
9 Massachusetts, USA.

10

11 **2** Community Ecology Unit, Swiss Federal Institute for Forest, Snow and Landscape Research WSL, CH-8903
12 Birmensdorf, Switzerland

13

14 **3** Plant Ecology Research Laboratory PERL, School of Architecture, Civil and Environmental Engineering ENAC,
15 EPFL, CH-1015 Lausanne, Switzerland

16

17 **4** Department of Biogeochemical Signals, Max-Planck-Institute for Biogeochemistry, Jena, Germany.

18

19 **5** Section Systems Ecology, Amsterdam Institute for Life and Environment, Vrije Universiteit Amsterdam, The
20 Netherlands

21

22 **6** Laboratorio de Biodiversidad y Funcionamiento Ecosistémico, Instituto de Recursos Naturales y Agrobiología
23 de Sevilla (IRNAS), CSIC, Sevilla, Spain

24

25 **7** CREAM, E08193 Bellaterra (Cerdanyola del Vallès), Catalonia, Spain.

26

8 Forestry and Game Management Research Institute, Strnady 136, Jíloviště 252 02, Czech Republic.

27

9 State Key Laboratory of Efficient Production of Forest Resources, Beijing Forestry University, Beijing 100083,
28 China

29

10 Lancaster Environment Centre, Lancaster University, Lancaster, UK

30

11 Birmingham Institute of Forest Research, University of Birmingham, United Kingdom

32

12 School of Biosciences, Edgbaston Campus, University of Birmingham, United Kingdom

34

13 Department of Agroecology, Climate and Water, Aarhus University, 8830 Tjele, Denmark

36

14 Department of Environmental Studies, New York University, New York, NY 10012, USA.

38

15 Santa Fe Institute, New Mexico, NM 87501, USA

40

Correspondence to: Helena Vallicrosa (helena.vallicrosa@gmail.com)

42

43 **ABSTRACT**

44

45
46 The role of plants in sequestering carbon is a critical component in mitigating climate
47 change. A key aspect of this role involves plant nitrogen (N) uptake (Nup) and N use
48 efficiency (NUE), as these factors directly influence the capacity of plants to store carbon.



49 However, the contribution of N deposition and soil factors (biotic and abiotic) in addition to
50 climate to plant N cycle, remains inadequately understood, introducing significant
51 uncertainties into climate change projections. Here, we used ground-based observations
52 across 159 locations to calculate Nup and NUE and identify their main drivers in natural
53 ecosystems. We found that global plant Nup is primarily driven by N deposition, air
54 temperature and precipitation, with Nup increasing in warmer and wetter areas. In
55 contrast, NUE is driven by soil biotic and abiotic factors, with little direct control by climatic
56 factors. Specifically, NUE decreased with the intensity of the colonization by arbuscular
57 mycorrhizal fungi and increased with soil pH and soil microbial stocks. Nup and NUE
58 presented opposite latitudinal distributions, with Nup higher on tropical latitudes and NUE
59 higher towards the poles. Total soil N stocks were not found to be a driver of Nup or NUE.
60 We also compared our results with TRENDY models and found that models may
61 overestimate Nup by $\sim 100 \text{ Tg N yr}^{-1}$ in the tropics and triple the standard deviation on
62 boreal latitudes. Our findings emphasize the effect of N deposition and soil microbes that,
63 in addition to climate and soil pH, are crucial for accurately predicting ecosystems' capacity
64 to sequester carbon and mitigate climate change.

65

66 Plain language summary

67 We used field empirical data worldwide to calculate plant nitrogen uptake (Nup) and
68 nitrogen use efficiency (NUE) in woodlands and grasslands and determine its drivers, which
69 can be used as empirical validation for models. Even though some regions of the world have
70 decreased their N deposition, N deposition is still the most important driver explaining plant
71 nitrogen uptake, aside from climatic variables.

72

73

74

75

76

77

78

79

80

81

82

83

84

85

86

87

88

89

90

91

92



93

94

95

96

1. Introduction

97

98 Climate and nutrient availability play significant roles in the capacity of plants to sequester
99 carbon (C). Nitrogen uptake (Nup) and nitrogen use efficiency (NUE) are fundamental
100 processes in plant-soil N cycling, which in turn impact biodiversity, ecosystem productivity,
101 C sequestration, food security and human health (Peñuelas et al., 2020). Hence, realistic
102 quantifications of Nup and (NUE) and the understanding of their drivers are crucial to
103 predict the fate of terrestrial ecosystems under a changing environment. Climate, biomass
104 production, and Nup are strongly intertwined, where hotter and wetter ecosystems have
105 the capacity to grow more, increase their N demand and therefore absorb more N if
106 available (Berntson et al., 1998; Wu et al., 2011). Nonetheless, several factors can affect N
107 availability. Traditionally, total soil N stocks were used to proxy N availability or plant Nup.
108 Although this correlation is weak, it is still used in a modeling perspective (Stevens et al.,
109 2015; Vicca et al., 2018) assuming that total soil N, positively correlates with N availability.
110 Recent advances in plant-soil science revealed the remarkable importance of the soil biotic
111 community in N availability related processes and plant growth (Aber et al., 2001;
112 Sinsabaugh et al., 2002; Sinsabaugh et al., 2008; Crowther et al., 2019; Delgado-Baquerizo
113 et al., 2020; Etzold et al., 2020). Thus, by extension, soil microorganisms (e.g., soil microbes
114 stocks and mycorrhizal associations) could potentially affect Nup and NUE. In addition, N
115 deposition has increased from ~30 to ~80 Tg N/year worldwide since 1850 (Kanakidou et
116 al., 2016), with substantial effects on global biogeochemical fluxes and N availability (Elser
117 et al., 2010; Batty et al., 2017; Peñuelas et al., 2020). Consequently, reliable quantifications
118 of plant Nup and NUE need to include climatic factors as well as soil biotic factors and N
119 deposition.

120

121 N regulates the capacity of ecosystems to store C (Hungate et al., 2003; Fernández-Martínez
122 et al., 2014; 2019; Wang et al., 2017) and respond to climate change drivers (Fleischer et
123 al., 2019; Terrer et al., 2019; Walker et al., 2021; Zhou et al., 2022) being the C-N assembly
124 relevant for land surface models (LSM). Eight of the LSM of the TRENDY ensemble (Sitch et
125 al., 2015), a model ensemble designed to disentangle the effects of climate, CO₂, land-use
126 and land cover change, include representations of the N cycle and plant N uptake.
127 Nonetheless, its parameterization of N cycling is poorly constrained by observations (Zaehle
128 et al., 2014; Fowler et al., 2015; Braghieri et al., 2022). As a consequence, when models are
129 assembled, the result leads to accumulated uncertainty (Prentice et al., 2015; Franklin et
130 al., 2020) and therefore divergent predictions of the land sink (Zaehle et al., 2014; Stocker
131 et al., 2016; Arora et al., 2020). Furthermore, when accounting for N interactions, LSM do
132 generally not consider the direct effects of microorganisms' missing out on the role of soil
133 bacteria or mycorrhizae on plant nutrient uptake. Thus, including global calculations of
134 plant Nup and NUE based on empirical data as well as accounting for climate, N deposition,
135 and soil biomass interactions would potentially refine the N accountability in LSM.

136



137 Here, we gathered information from 159 plots worldwide that describe woodlands and
138 grasslands across different biomes to calculate plot-based plant Nup and plant NUE using
139 exclusively empirical field data. Our analyses combine N concentration and net primary
140 productivity (NPP) data in different aboveground and belowground plant tissues (i.e.,
141 leaves, roots, stem). We used linear models to identify the drivers of Nup and NUE, including
142 N deposition, soil microbes, woodiness and climatic factors. We then upscaled those results
143 using the machine-learning models to quantify yearly plant Nup and plant NUE at a global
144 scale in natural terrestrial ecosystems (woodlands and grasslands) and compared these
145 results with simulations from LSM. We hypothesize that factors such as N deposition and
146 soil microorganisms have significant impacts on Nup and NUE respectively, playing a role as
147 important as climatic drivers. We expect the ground-based data, and incorporation of these
148 N-relevant drivers to increase the accuracy of global Nup quantifications. Thus, a mismatch
149 between our estimation and current TRENDY simulation outputs is expected.

150

151 **2. Results and discussion**

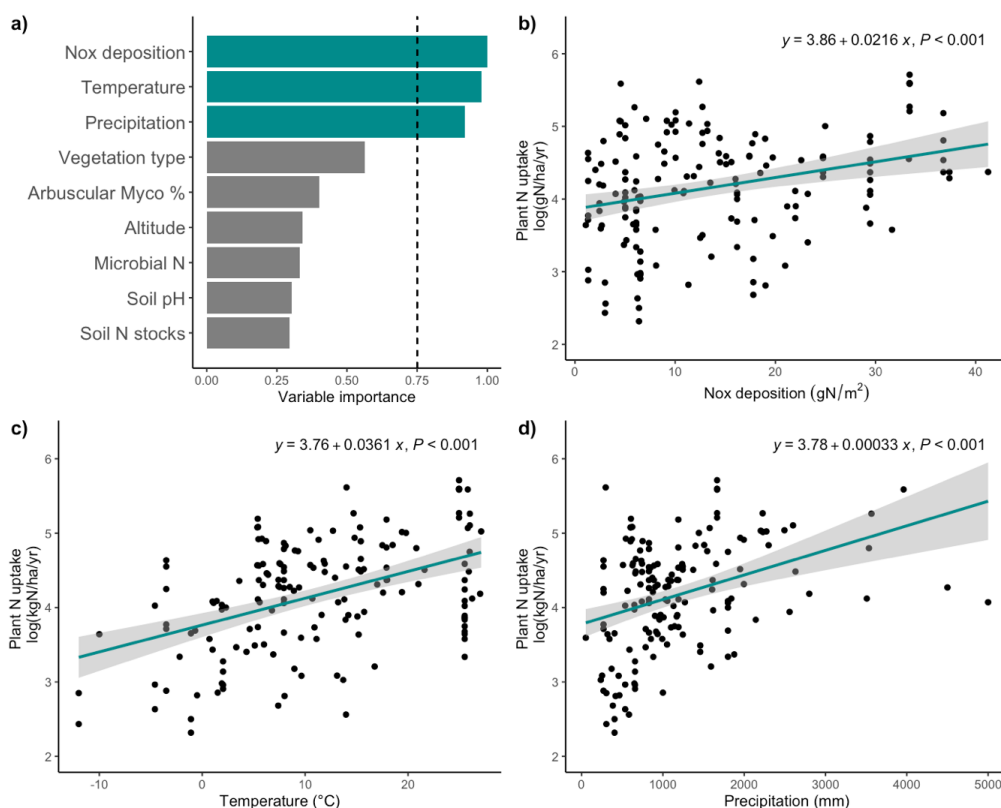
152 **2.1 Nitrogen uptake and nitrogen use efficiency**

153 Our findings indicate that N deposition and climate are fundamental factors explaining plant
154 Nup on a global scale (Fig. 1). Further analysis revealed a positive relationship between Nup
155 and accumulated N deposition, mean annual temperature (MAT), and mean annual
156 precipitation (MAP). Thus, regions that are warm and wet, and also experience higher levels
157 of N deposition, exhibit the highest rates of Nup. Our empirical results did not show
158 important relationships between plant Nup and soil microbial interactions nor soil physico-
159 chemical variables including soil N stocks at a global scale (Fig. 1a). We further tested the
160 univariate relation between Nup and total soil N stocks with no significant relation among
161 them (Fig. S1a).

162



Plant nitrogen uptake



163
164
165
166
167
168

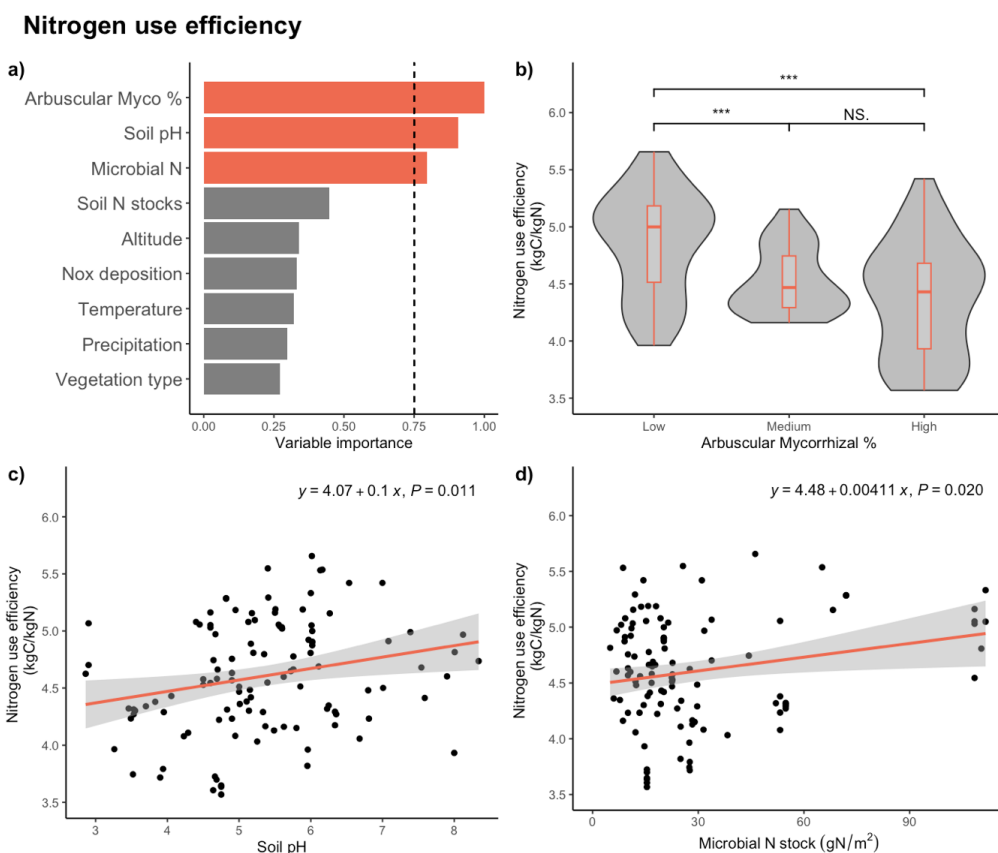
Figure 1. a) Variable importance plot for the general linear model describing plant nitrogen uptake (Nup). The dashed line is set at 0.8, separating the threshold for important variables. The model pseudoR2 was 0.349. Linear regressions were displayed describing plants' nitrogen and important variables b) accumulated Nox deposition from 1901 to 2021, c) mean annual temperature, and d) mean annual precipitation. Equation and p-value per regression displayed. Acronyms: Nox: oxidized nitrogen, N: nitrogen, Myco %: Mycorrhizal percentage.

169
170
171
172
173
174
175
176

In contrast, when describing NUE our model selection analysis identified soil biotic and abiotic factors as NUE drivers with little direct control by climatic factors (Fig. 2). Specifically, our results described NUE decreased with AM % but a positive relation between soil pH, soil microbial N stocks and NUE was found. Thus, when plant species are more colonized by arbuscular mycorrhizae, are less efficient in N use to build biomass. In contraposition, basic pH and abundant soil microbial stocks facilitate higher NUE rates. Even though soil variables appear to be important for NUE, soil N stocks remain unrelated to NUE in the model and when tested individually (Fig. S1b).



177



178

179

180

181

182

183

Figure 2. a) Variable importance plot for the generalized linear model describing nitrogen use efficiency (NUE). The model $\text{pseud}R^2$ was 0.355. The dashed line is set at 0.75, separating the threshold for important variables. In b) arbuscular mycorrhizae percentage is divided into low, medium, and high, and NUE is displayed. * = P-value < 0.05, ** = P-value < 0.01, *** = P-value < 0.001. Linear regressions were displayed describing plants' nitrogen use efficiency c) soil pH and d) microbial N stocks. Equation and p-value per regression displayed.

184

2.2 Global maps of Nup and NUE

185

186

187

188

189

190

191

192

193

194

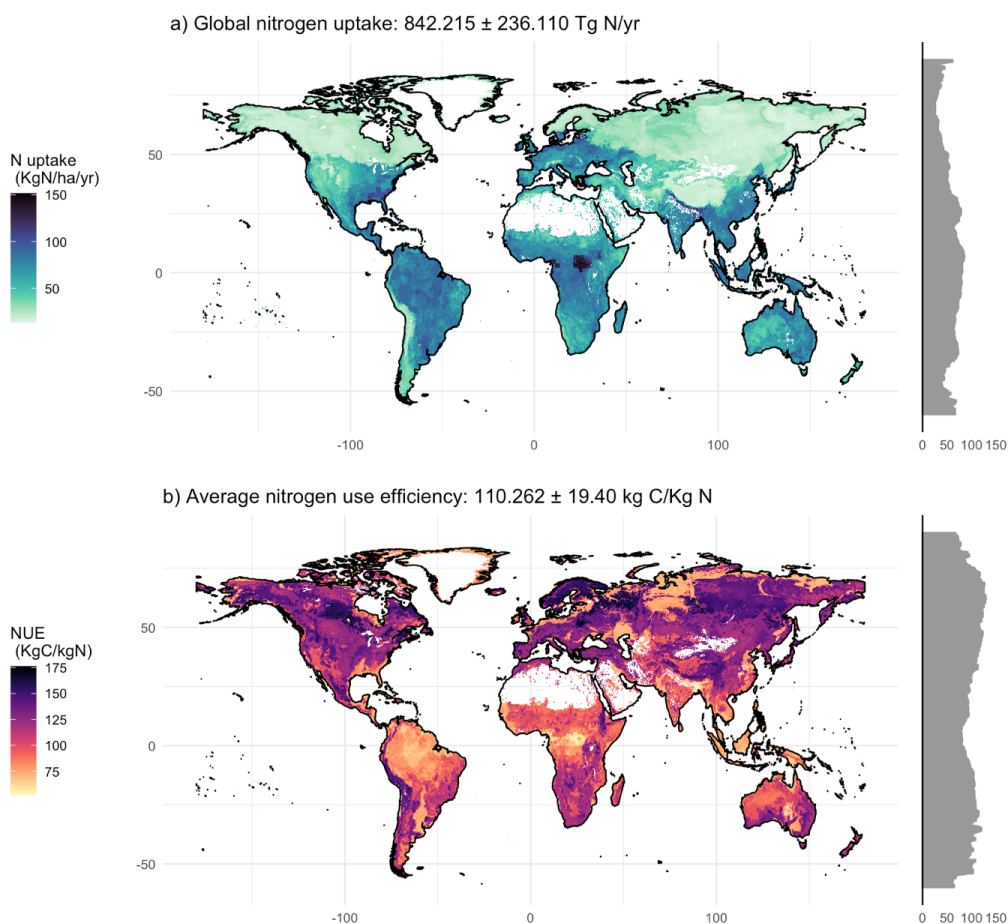
195

196

Next, we used a machine-learning model to understand the global magnitude and distribution of Nup and NUE when the relationships found at the site-level are extrapolated at a global scale. For methodological consistency, the XGBoost model was trained using the same nine variables as the linear model. We identified temperature, precipitation, and N deposition as the most critical factors for describing Nup (Fig. S2), which aligned with those in the linear model, albeit in a slightly different order. Partial dependence plots further corroborated these relationships, showing consistent correlation signs with those observed in the linear models (Fig. S3). The upscaled Nup map showed a total yearly Nup of 842.215 ± 236.11 Tg of N, with a mean coefficient of variation of 26.77 % (Fig. S4) and an r^2 of 0.54 (Fig. S2). The lowest Nup values were on boreal latitudes and mountain ranges such as the Rocky Mountains in the USA, the Andes in South America, the different mountain ridges in Europe, and the Himalayan plateau in Asia. The higher rates of Nup are predicted in



197 temperate latitudes in Europe, the eastern United States, Southeast Asia, East Australia,
198 most of South America and central Africa, with the most intense spot around Congo, where
199 there is the most N deposition, temperature and precipitation combined (Fig. 3a).
200 Therefore, Nup map shows an NPP influence, driven by temperature and precipitation, but
201 added to an N deposition distribution that shades the strictly latitudinal distribution of Nup.
202



203
204
205
206
207

Figure 3. Upscaled global maps describing a) Plant nitrogen uptake and b) Nitrogen use efficiency. The total amount of nitrogen uptake calculated per year is 842.215 Tg of N with a standard deviation of ± 236.11 . The mean value of global nitrogen use efficiency is 110.26 kg of C per kg of N, and its standard deviation is 19.40. White color describes no data due to a lack of grasslands or woody vegetation.

208 The machine-learning models describing NUE showed the importance of microbial N stocks,
209 altitude, precipitation, soil pH, and AM% as NUE drivers (Fig. S5). These results generally
210 align with the variable importance shown in the linear models, with the addition of
211 precipitation and altitude. The variables' relation showed similar general trends as in the
212 linear model (Fig. S6). The average predictions for NUE at a global scale were 110.262 units
213 of C per unit of N with a mean coefficient of variation of 17.89 % (Fig. S4) and an r^2 of 0.44



214 (Fig. S5). The map distribution showed general lower NUE around the Equator, and
215 progressively increasing towards the poles. Nonetheless, some heterogeneous patches
216 alternating high and low NUE can be found between 50 and 60 degrees latitude north (Fig.
217 3b).

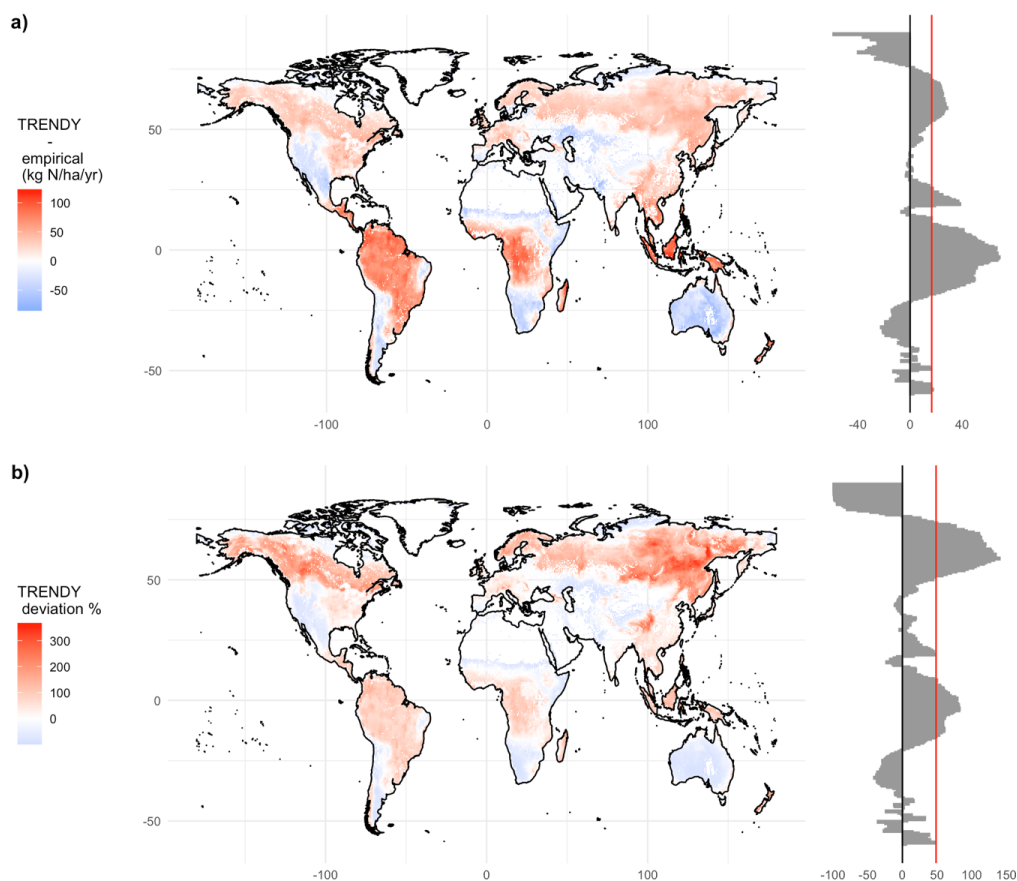
218

219 **2.3 Global-scale Nup comparison with TRENDY models**

220 We further seek to compare our estimates for the total yearly Nup upscaled from field
221 observations with the mean of the Nup provided by the eight models included in TRENDY.
222 When comparing TRENDY Nup with our Nup upscaled projections, we found clear
223 geospatial pattern differences. TRENDY models produce higher Nup in the tropical regions,
224 reaching differences of around $100 \text{ kg N ha}^{-1} \text{ yr}^{-1}$ in those areas (Fig. 4a) representing more
225 than 100% of the Nup estimated by field observations (Fig. 4b). Other areas like the north
226 and northeast of North America, Southeast Asia, and north of Eurasia also appear to have
227 higher Nup values in TRENDY models than in field observations. In boreal latitudes, the
228 TRENDY models deviation for Nup could even reach 300% of overestimation. On the other
229 hand, areas where the upscaled approach projects higher values than the TRENDY models,
230 are the austral latitudes, the Middle Eastern regions, the Somali peninsula, and the Rocky
231 Mountains (Fig. 4). Overall, TRENDY models estimate higher values of Nup, by 16.61 kg N
232 $\text{ha}^{-1} \text{ yr}^{-1}$, meaning the 48.54 % of the variability. When aggregating the total year Nup, LPX-
233 Bern and CLM5.0 were the models that predicted overall values exceeding our range of
234 confidence, assuming a significantly larger Nup (Fig. S7).

235

236



237

238

239

240

241

242

Figure 4. Comparison between the mean of the nitrogen uptake provided by TRENDY v8 models minus the upscaled nitrogen uptake. The red color stands for higher values on the TRENDY model, and the blue color stands for higher nitrogen uptake values on the upscaled approach. In a) units in kg N ha⁻¹ yr⁻¹ and in b) units in percentage of deviation from field upscaling. Latitudinal aggregation on the right, with a red vertical line showing a) the mean of the total comparison at 16.61 kg N ha⁻¹ yr⁻¹ and b) the mean percentage of deviation at 48.54%.

243

2.4 Nup global drivers and implications

244

245

246

247

248

249

250

251

252

253

254

255

Our models estimated the annual global plant Nup at 842.215 ± 236.110 Tg of N. This figure is consistent with the findings of Peng et al., 2023, which estimated 950 ± 260 Tg of N, and Braghieri et al., 2022, with an estimated uptake of 841.8 Tg N. The slight variations can be attributed to differences in methodologies and data sources (simultaneous plot-averaged records vs individual-level records) used in these studies. In our study, linear models and machine learning models are consistent when determining N deposition, temperature, and precipitation as global drivers of Nup. Hotter and wetter environments increase biological activity, leading to more biomass production and therefore more N demand. An increase in N demand with enough N availability is associated with an increase in Nup. The accumulation of N deposition throughout time originating from anthropogenic sources has been increasing the N availability in some areas, generally close to industrial or agroforestry pools. Hence, in a global change context where CO₂ fertilization and temperature increase



256 have generated a greening effect (Ruehr et al., 2023), areas with higher N deposition were
257 able to better supply the increasing N demand. Thus, according to our results,
258 anthropogenic N supply may have become a Nup driver as important as climate.

259

260 These results are concerning since our data emphasize the far-reaching influence of human-
261 induced nitrogen deposition in shaping global Nup patterns. Some regions such as Europe,
262 the Eastern USA, and the tropics have decreased their N deposition during the last four
263 decades (Ackerman et al., 2019). Nonetheless, these efforts do not translate yet on low N
264 deposition effects in natural woodlands and grasslands. This sustained entrance of
265 anthropogenic N has been associated with a fertilization effect, enhancing the land C sink
266 by $0.72 \text{ Pg C yr}^{-1}$ during the 2010s (Gurmesa et al., 2022). Nonetheless, this N fertilization
267 effect showed evidence of saturation in forests and grasslands (Tian et al., 2016; Peng et al.,
268 2020), where the biomass production and therefore the C sink increase slowed down.
269 Consequently, this input of N not being captured by biomass will enhance the N leaching
270 associated with eutrophication, acidification, loss of biodiversity, and N_2O emissions (Aber
271 et al., 1989; Gundersen et al., 1998; Bobbink et al., 2010) exacerbating environmental
272 problems.

273

274

2.5 NUE global drivers and implications

275

276 Our results predict a mean NUE of $110.262 \pm 19.40 \text{ kg C per kg N}$. Our results indicate soil
277 biotic and abiotic factors drive NUE in natural ecosystems. The main divergence between
278 linear models and machine learning models is the importance of altitude and precipitation,
279 which showed explicit relevancy only in machine learning models. We attribute these
280 differences to the nature of the models, where machine-learning models accommodate
281 correlations without modifying their variable importance. Thus, the important variables in
282 the linear model could also have embedded important latitudinal gradients and therefore
283 altitudinal or precipitation gradients. Our NUE predictions contrasted with Peng et al., 2023,
284 which predicts a mean NUE of $76 \pm 26 \text{ kg C per kg of N}$. The main difference between studies
285 is that our approach included biotic factors, such as mycorrhizal associations and microbial
286 interactions, that described NUE better than abiotic factors. In contrast, Peng et al., 2023
287 focused their predictions only on abiotic factors. In that regard, we do not consider
288 environmental variables such as precipitation to be totally detached from NUE relations,
289 since they are somewhat drivers of important biotic variables such as AM %, soil pH, and
290 microbial N stocks. Nonetheless, the results showed that including biotic variables may
291 result in more efficient use of N by plants at global scale.

291

292 The response of NUE has been postulated as a method to assess N saturation in plant
293 communities (Shcherbak et al., 2014). A negative relation between N addition and NUE and
294 lower NUE levels would indicate N saturation (Iversen et al., 2010). In our study, tropical
295 areas are shown to have the lowest NUE, being the less N limited and matching with
296 previous global upscaling studies using different approaches (Du et al., 2020; Vallicrosa et
297 al., 2022). According to the soil age hypothesis (Walker and Syers, 1976), N accumulates in
298 ecosystems through time due to biological processes. Thus, newer formation areas, such as
299 high elevation or lower pH areas are those showing higher values of NUE and where N is



300 expected to be more limiting. Our results only show a modest effect of N saturation due to
301 N deposition, so further studies are needed to better assess where and under what
302 circumstances areas are N saturated due to N deposition.

303

304 Biological activity, such as the type of mycorrhizal associations and soil microbes N stocks,
305 was found to have a strong impact in the terrestrial N cycle. Arbuscular mycorrhizal
306 associations are the most abundant in the tropics (Soudzilovskaia et al., 2019) and are
307 theorized to be more efficient in nutrient capture and more abundant in areas with fast N
308 cycling (Averill et al., 2019). Our models show that AM associations have lower NUE,
309 possibly driven by the abundance of N and the high efficiency of AM associations in N
310 acquisition. Conversely, N obtention was more efficient in areas with high soil microbes
311 stocks. As described by Kuzyakov and Xu 2013, we hypothesize a potential competition
312 effect between soil microbes and plants for N, but further studies are needed to
313 corroborate this relation. Thus, given the importance of biological activity in fixing and
314 transforming N, it is reasonable that total soil N stocks, that include N in all forms and
315 aggregations, would not be a good indicator of N availability and plant N uptake.

316

317 **2.6 Discrepancies between Nup map and TRENDY**

318 TRENDY model ensemble projects substantially higher Nup values than the empirical
319 upscaling. These differences were especially relevant in the tropics in absolute terms and in
320 boreal latitudes in % of deviation. This mismatch could be associated with an
321 overestimation of terrestrial C sink capacity and a misinterpretation of the role of
322 vegetation in N cycling. A possible explanation of this phenomenon would be the
323 overestimation of biomass production by LSM when not accounting for growth-limiting
324 factors such as phosphorus availability, drought, or overall biotic competition. Alternatively,
325 overestimation when accounting for N concentration in tissues could also lead to Nup
326 overestimation, which would necessarily reflect in overall lower NUE values. In our
327 calculations, we embraced the variability of N concentration and net primary productivity
328 among tissues and leaf resorption to generate a truthfully Nup and NUE values.

329

330 **2.7 Representativity and future research**

331 An inherent challenge in ecological studies of this scale is to ensure the global
332 representativeness of the dataset, since there are systematic geographical sampling biases
333 underrepresenting the global south. In this study, the 28 % of the data comes from areas
334 below 15° latitude, outside the US, Europe, or China (Fig. S8). When accounting for
335 ecosystems representativity, the Whittaker diagram shows we have a representation of all
336 the biomes (Fig. S9), showing the lowest representativity on subtropical desert, tundra, and
337 temperate rainforest. Nonetheless, we acknowledge that calculations based on empirical
338 data, especially when a portion of the data have undergone a gap-filling process, can still
339 have biases associated with sampling and the upscaling process, which are mainly defined
340 by the more represented biomes of the observations. Still, we believe that calibrating and
341 cross-checking models built over mathematical assumptions with field measurements is
342 necessary to better root models to reality.

343



344 This study is focused on a quantitative approach at global scale, attempting to target
345 variables' relative importance on Nup and NUE along with its correlations to environmental
346 and biotic variables. In future research, specific data detailing the different N fractions
347 obtained at a global scale (e.g. organic-inorganic, ammonium-nitrate) and a more
348 mechanistic frame are strongly encouraged. Approaches such as in Niu et al., 2016
349 quantifying the fraction of Nup taken by plants, leached and retained in the soil at a global
350 scale are crucial to enhance our understanding of the N cycle and its interactions with
351 ecosystems.

352

353 **3. Conclusion**

354 We showed that accumulated N deposition and climatic variables are the main global-scale
355 factor describing Nup, where regions that are warm and wet and also experience higher
356 levels of N deposition, exhibit the highest rates of Nup. This result highlights the far-
357 reaching influence of nitrogen deposition in shaping the global Nup pattern. Interestingly,
358 NUE was shown to be driven by soil biotic and abiotic factors, emphasizing the importance
359 of soil microorganisms and pH as regulators of the N cycle. We further revealed that total
360 soil N stocks are not a Nup nor NUE driver. Our upscaling showed large spatial-explicit
361 differences with TRENDY Nup values, where TRENDY projects higher absolute values around
362 the tropics and higher deviation values in boreal latitudes. This mismatch in the spatial
363 correlation between empirical data and land system models could substantially affect
364 model accuracy and future predictions of the C sink, where the tropical capacity to store C
365 might have been overestimated. Our results provide insights to understand better the C –
366 N interactions, N cycling, and absorption in terrestrial ecosystems and highlight that N
367 deposition largely impacts plant Nup worldwide.

368

369 **4. Methods**

370 **4.1 Plant data gathering**

371 We gathered 159 (Table S1) field plot data in natural conditions, including dominant species
372 and vegetation type (grassland, coniferous or broadleaved), foliar and root N concentration,
373 foliar and root biomass production, and stem biomass production in the case of woody
374 plants on the same location and time. In situ measurements for foliage and fine roots are
375 the most relevant for Nup calculation (Dybzinski et al., 2024), so all our datapoints include
376 biomass production (NPP) and N content (N%) of leaves and roots. We gathered 45
377 datapoints, representing a 28% of the data, coming from latitudes under the 15° latitude,
378 despite of the systematic lack of field sampling on some regions of the earth such as the
379 global south. We also complemented the dataset with field values of litter biomass
380 production, litter N concentration, stem N concentration, soil pH, soil C %, soil N %, soil
381 texture, soil moisture, mean annual precipitation, mean annual air temperature, and
382 altitude. We included woody and grassland natural environments (Fig. S8), including
383 representation from most biomes according to Whitaker's diagram (Fig. S9). Each data
384 point covered by the analysis has been collected from 1984 to 2022. If stem N was missing,
385 happening in 25% of the data entries, we gap-filled it with the mean value of its vegetation
386 type (coniferous=0.33 or broadleaved=0.52%). With leaves, stem and roots we calculated
387 the gross Nup (see in the next section). By subtracting the amount of N recovered during



388 leaf senescence we obtain the net Nup. If litter biomass was missing, 52% of the time, we
389 assumed it to be the same amount of green leaf biomass production. If litter N
390 concentration was missing, we calculated the net Nup using the predicted value from a
391 linear model created with net Nup in the base of gross Nup, in 33% of the entries. This
392 model had an r2 of 0.88, a p-value < 2.2e-16, and a correlation of 0.72 between gross and
393 net Nup.

394

395 **4.2 Environmental data**

396 We extracted mean annual precipitation from WorldClim2 (Fick and Hijmans, 2017), as well
397 as soil pH, soil C, and soil N, soil moisture, soil bulk density, and soil texture from soilGrids
398 (Poggio et al., 2021). All soil data for the topsoil layer (0-15 cm). We also identified the
399 potential mycorrhizal association from the dominant species based on Soudzilovskaia et al.
400 2020, and categorized it into 0, 50, or 100 arbuscular mycorrhizal (AM) percentages. When
401 dominant species were not provided, we extracted the AM% based on the AM map of
402 Soudzilovskaia et al. 2019 and the coordinates of our samples. Moreover, we extracted the
403 microbial N stock from Xu et al. 2013. We calculated and obtained the accumulated oxidized
404 N deposition from Yang and Tian, 2022 from 1901 to 2022 by georeferencing each field plot.
405 Oxidized and reduced N deposition are correlated and are thought to have similar ecological
406 effects (Sutton and Fowler, 1993; Yang and Tian, 2022). Oxidized forms generally come from
407 combustion reactions while reduced forms generally come from agricultural practices. We
408 decided to use the oxidized form because it is the most equally distributed at a global scale.

409

410 **4.3 Nitrogen uptake calculation**

411 We calculated the increase in annual N stock for each tissue (leaves, stem, roots, and litter)
412 by multiplying the biomass increase by its N concentration. We obtained the gross annual
413 Nup by aggregating tissue's Nup (roots, leaves, and stem if woody). To account for the N
414 that has been reabsorbed before senescence, we subtracted the litter N stock from the
415 green leaves N stock. We subtracted the reabsorbed N from the gross Nup to obtain the
416 final net Nup value as follows:

417

$$418 \quad \text{GrossNup} = (\text{NPPleaves} * \text{Nleaves} + \text{NPPstem} * \text{Nstem} + \text{NPProots} * \text{Nroots})$$

419

$$420 \quad \text{NetNup} = \text{GrossNup} - (\text{NPPleaves} * \text{Nleaves} - \text{NPPlitter} * \text{Nlitter})$$

421

422 *Nup* = Plant nitrogen uptake (kg N/ha/yr)

423 *NPP* = Net primary production (kg N/ha/yr)

424 *N* = Nitrogen (% of dry weight)

425

426 **4.4 Nitrogen use efficiency calculation**

427 We calculated the nitrogen use efficiency (NUE) by calculating the total amount of biomass
428 produced in leaves, stems, and root tissue divided by the amount of nitrogen in each tissue.
429 It will give the amount of biomass produced by a unit of nitrogen.

430

$$431 \quad \text{NUE} = (\text{NPP}_{\text{leaves}} / \text{Nup}_{\text{leaves}}) + (\text{NPP}_{\text{stem}} / \text{Nup}_{\text{stem}}) + (\text{NPP}_{\text{roots}} / \text{Nup}_{\text{roots}})$$

432



433 *NUE* = Nitrogen use efficiency (kg C / kg N)
434 *NPP* = Net primary production or biomass increase (kg N/ha/yr)
435 Nup = Nitrogen uptake by tissue calculates as $NPP * N \%$
436

437 **4.5 Linear statistical analysis**

438 From the available variables collected, we selected the less correlated ones using the *cor*
439 function in R to deal with multicollinearity. The less correlated variables selected were mean
440 annual air temperature, mean annual precipitation, altitude, arbuscular mycorrhizae
441 percentage, microbial N stock, soil N stock, soil pH, accumulated oxidized N deposition from
442 1901 to 2022, and woodiness. The biggest collinearity among variables was 0.52 between
443 mean annual temperature and AM presence (Table S2). Generalized linear models were
444 created using Nup and NUE as dependent variables and the family was set up as Gamma
445 with an inverse link to fulfill the residuals normality requirements. We performed a model
446 selection using the *dredge* function in the MuMIn R package (Barton, 2023) and chose the
447 best linear model based on its lowest AIC. We calculated the variable importance using the
448 function *sw* on the MuMIN R package (Barton, 2023). We calculated the pseudo R square
449 of the models using the function *pR2* from the package *pscl* (Jackman, 2020). Figures were
450 created using the R package *ggplot2* (Wickham, 2016).
451

452 **4.6 Nitrogen uptake and nitrogen use efficiency upscaling**

453 To upscale Nup and NUE to global grasslands and woody vegetation, we used extreme
454 gradient boosting (XGBoost) models splitting the database into train, test, and validation
455 using a ratio of 70:20:10, respectively. Extreme gradient boosting is a machine learning
456 algorithm that builds ensemble decision trees, applying regularization and pruning
457 techniques to improve performance and prevent overfitting (Chen et al., 2016). We trained
458 an XGBoost model using the R package *xgboost* (Chen et al., 2023), forcing an early stop
459 based on minimum root mean squared error to avoid overfitting and setting up the
460 objective as a gamma regression. We optimized the parameters based on performance at a
461 maximum depth of 6, minimum child weight of 1, and eta of 0.3. We considered the same
462 independent variables included in the linear model without interactions. We repeated this
463 process 20 times with random database separation to stabilize the variability due to
464 randomness in subset splitting. We extracted the variable importance of each model using
465 the function *xgb.plot.importance* on the *xgboost* R package (Chen et al., 2023), calculated
466 the mean of the values among the 20 different training sets, and displayed it using *ggplot*.
467 We calculated partial dependence plots using the function *partial* in *purrr* R package
468 (Wickham and Henry, 2023) to explore the non-linear relations on the models. To calculate
469 the model performance, we calculated the mean squared error of the test set and the r
470 squared of the predicted vs observed in the validation subset, considering the validation set
471 as completely independent.
472

473 To predict the values at a global scale, we used the spatial explicit mean annual
474 precipitation, mean annual temperature, and altitude variables provided by WorldClim2
475 (Fick and Hijmans, 2017); the microbial N stocks by Xu et al. 2013; the oxidized accumulated
476 N deposition from 1909 to 2022 calculated from Yang and Tian 2022 and soil N stocks and



477 soil pH provided by soilGrids 2.0 (Poggio et al., 2021) at 15 cm depth. We reclassified the
478 European Space Agency Land Cover (ESA-LC) map (Defourny, 2019) (Table S3) and we
479 downscaled its resolution to 2 km using the raster R package (Hijmans, 2023). We upscaled
480 each of the 20 Nup and NUE models using the trained XGBoost models and their prediction
481 per pixel at 2 km resolution and calculated the mean to obtain the final maps. We
482 parallelized the process using the *parallel* function and *spaDES.tools* R package (McIntire
483 and Chubaty 2023) to accelerate the upscaling. We masked areas not considered woodlands
484 or grasslands in natural conditions according to the European Space Agency cover map
485 (Defourny, 2019) (Table S3), and then, we obtained a map of the yearly Nup, Nup standard
486 deviation, and annual NUE. We obtained the final number of yearly Nup by summing all the
487 pixels available.

488

489 **4.7 Nitrogen uptake comparison with TRENDY models ensemble**

490 We obtained the available Nitrogen uptake of Vegetation (fNup) variable associated with
491 all the available models in TRENDY v8 S3 (Sitch et al., 2015; Le Quéré et al., 2018). The
492 models containing fNup are ORCHIDEE, LPX-Bern, LPJ-GUESS, JULES, JSBACH, DLEM,
493 CLM5.0, and Cable-POP, and the S3 experiment in the simulation considering the adaptation
494 of CO₂, land use, N deposition, and climate from 1850 representing current environmental
495 conditions. We calculated the yearly mean Nup from 1984 to 2022 for each model. Then,
496 we calculated the difference between each TRENDY model and our Nup estimations. We
497 also calculated the latitudinal mean of the difference to achieve a latitudinal profile and
498 calculated the overall mean.

499

500 **Contributions**

501 H.V. and C.T. conceived the project; C.T. got the funding and supervised the work; H.V.,
502 C.M., A.K., J.C., and D.T. collected and compiled the data; H.V. curated and analyzed the
503 data, created the visuals and wrote the first draft; H.V., C.T., M.D.B., M.F.M., M.L., D.G.,
504 contributed with substantial ideas and feedback on the manuscript; all authors revised,
505 edited, and agreed on the final manuscript.

506

507 **Data availability statement**

508 The data gathered for this study, code and produced models are available at Zenodo
509 (Vallicrosa Pou, 2024).

510

511 **Competing interests**

512 The authors declare no competing interests

513

514 **Acknowledgments**

515 We acknowledge the members of the Terrer Lab for providing scientific consulting as well
516 as mental and emotional support during the investigation. We acknowledge the Pioneer
517 Center Land-CRAFT, Department of Agroecology, Aarhus University for making possible this
518 collaboration with D.G. J.C. was supported by the National Agency of Agricultural Research
519 of the Czech Republic (Project No. QK22020008) and the Ministry of Agriculture (CR),
520 institutional support MZE-RO0123, and he thanks FGMRI technician staff for help with field



521 and lab works. M.F.M was supported by the European Research Council project ERC-StG-
522 2022-101076740 STOIKOS and a Ramón y Cajal fellowship (RYC2021-031511-I) funded by
523 the Spanish Ministry of Science and Innovation, the NextGenerationEU program of the
524 European Union, the Spanish plan of recovery, transformation and resilience, and the
525 Spanish Research Agency.
526

527 References

- 528
529 Aber, J.D., Nadelhoffer, K.J., Steudler, P. & Melillo, J.M. (1989) Nitrogen saturation in northern forest
530 ecosystems. *BioScience*, 39, 378– 386.
531
532 Aber, J., and J. Melillo. 2001. *Terrestrial ecosystems*. Second edition. Harcourt Academic Press, San Diego,
533 California, USA.
534
535 Ackerman, D., Millet, D. B., & Chen, X. (2019). Global estimates of inorganic nitrogen deposition across
536 four decades. *Global Biogeochemical Cycles*, 33, 100– 107. <https://doi.org/10.1029/2018GB005990>
537
538 Arora, V. K., Katavouta, A., Williams, R. G., Jones, C. D., Brovkin, V., Friedlingstein, P., et al. (2020). Carbon-
539 concentration and carbon-climate feedbacks in CMIP6 models and their comparison to CMIP5 models.
540 *Biogeosciences*, 17(16), 4173–4222. <https://doi.org/10.5194/bg-17-4173-2020>
541
542 Averill, C., Bhatnagar, J. M., Dietze, M. C., Pearse, W. D. & Kivlin, S. N. Global imprint of mycorrhizal fungi
543 on whole-plant nutrient economics. *Proc. Natl Acad. Sci. USA* 116, 23163–23168 (2019).
544
545 Bartoń K (2023). *_MuMIn: Multi-Model Inference_*. R package version 1.47.5, <[https://CRAN.R-](https://CRAN.R-project.org/package=MuMIn)
546 [project.org/package=MuMIn](https://CRAN.R-project.org/package=MuMIn)>.
547
548 Bauters, M., Verbeeck, H., Rütting, T., Barthel, M., Bazirake Mujinya, B., Bamba, F., Bodé, S., Boyemba, F.,
549 Bulonza, E., Carlsson, E., Eriksson, L., Makelele, I., Six, J., Cizungu Ntaboba, L., & Boeckx, P. (2019).
550 Contrasting nitrogen fluxes in African tropical forests of the Congo Basin. *Ecological Monographs*, 89(1),
551 1–17. <https://doi.org/10.1002/ecm.1342>
552
553 Bauters, M., Janssens, I.A., Wasner, D. *et al.* Increasing calcium scarcity along Afrotropical forest
554 succession. *Nat Ecol Evol* 6, 1122–1131 (2022). <https://doi.org/10.1038/s41559-022-01810-2>
555
556 BERNTSON, G.M., RAJAKARUNA, N. and BAZZAZ, F.A. (1998), Growth and nitrogen uptake in an
557 experimental community of annuals exposed to elevated atmospheric CO₂. *Global Change Biology*, 4:
558 607-626. <https://doi.org/10.1046/j.1365-2486.1998.00171.x>
559
560 Bobbink, R. *et al.* *Global assessment of nitrogen deposition effects on terrestrial plant diversity: a*
561 *synthesis. Ecol. Appl.* 20, 30–59 (2010).
562
563 Braghiere, R. K., Fisher, J. B., Allen, K., Brzostek, E., Shi, M., Yang, X., et al. (2022). Modeling global carbon
564 costs of plant nitrogen and phosphorus acquisition. *Journal of Advances in Modeling Earth Systems*, 14,
565 e2022MS003204. <https://doi.org/10.1029/2022MS003204>
566
567 Chen, T., and Guestrin, C. XGBoost: A scalable Tree Boosting System. arXiv:1603.02754v3
568



569 Chen T, He T, Benesty M, Khotilovich V, Tang Y, Cho H, Chen K, Mitchell R, Cano I, Zhou T, Li M, Xie J, Lin
570 M, Geng Y, Li Y, Yuan J (2023). `_xgboost: Extreme Gradient Boosting_`. R package version 1.7.5.1,
571 <<https://CRAN.R-project.org/package=xgboost>>.
572

573 Crowther TW, van den Hoogen J, Wan J, Mayes MA, Keiser AD, Mo L, et al. The global soil community and
574 its influence on biogeochemistry. *Science*. 2019;365:eaav0550.
575

576 Defourny, P. (2019): ESA Land Cover CCI project team; ESA Land Cover Climate Change Initiative
577 (Land_Cover_cci): Global Land Cover Maps, Version 2.0.7. Centre for Environmental Data Analysis, date
578 of citation. <https://catalogue.ceda.ac.uk/uuid/b382ebe6679d44b8b0e68ea4ef4b701c>
579

580 Delgado-Baquerizo M, Reich PB, Trivedi C, Eldridge DJ, Abades S, Alfaro FD, et al. Multiple elements of
581 soil biodiversity drive ecosystem functions across biomes. *Nat Ecol Evol*. 2020;4:210–20.
582

583 Du, E., Terrer, C., Pellegrini, A.F.A. et al. Global patterns of terrestrial nitrogen and phosphorus limitation.
584 *Nat. Geosci.* 13, 221–226 (2020). <https://doi.org/10.1038/s41561-019-0530-4>
585

586 Dyzbinski, R., Segal, E., McCormack, M.L. et al. Calculating Nitrogen Uptake Rates in Forests: Which
587 Components Can Be Omitted, Simplified, or Taken from Trait Databases and Which Must Be Measured In
588 Situ?. *Ecosystems* 27, 739–763 (2024). <https://doi.org/10.1007/s10021-024-00919-8>
589

590 Elser JJ, Fagan WF, Kerkhoff AJ, Swensson NG, Enquist BJ. 2010. Biological stoichiometry of plant
591 production: metabolism, scaling and ecological response to global change. *New Phytologist* 186: 593–
592 608.
593

594 Battye, W., Aneja, V.P. and Schlesinger, W.H. (2017), Is nitrogen the next carbon? *Earth's Future*, 5: 894-
595 904. <https://doi.org/10.1002/2017EF000592>
596

597 Etzold S, Ferretti M, Reinds GJ, Solberg S, Gessler A, Waldner P, Schaub M, Simpson D, Benham S, Hansen
598 K, Ingerslev M, Jonard M, Karlsson PE, Lindroos A-J, Marchetto A, Manninger M, Meesenburg H, Merilä P,
599 Nöjd P, Rautio P, Sanders TGM, Seidling W, Skudnik M, Thimonier A, Verstraeten A, Vesterdal L,
600 Vejrustková M, de Vries W (2020) Nitrogen deposition is the most important environmental driver of
601 growth of pure, even-aged and managed European forests. *Forest Ecology and Management* 458: 117762.
602 DOI: 10.1016/j.foreco.2019.117762
603

604 Fernández-Martínez, M., Vicca, S., Janssens, I. et al. Nutrient availability as the key regulator of global
605 forest carbon balance. *Nature Clim Change* 4, 471–476 (2014). <https://doi.org/10.1038/nclimate2177>
606

607 Fernández-Martínez, M., Sardans, J., Chevallier, F. et al. Global trends in carbon sinks and their
608 relationships with CO₂ and temperature. *Nature Clim Change* 9, 73–79 (2019).
609 <https://doi.org/10.1038/s41558-018-0367-7>
610

611 Fick, S.E. and R.J. Hijmans, 2017. WorldClim 2: new 1km spatial resolution climate surfaces for global land
612 areas. *International Journal of Climatology* 37 (12): 4302-4315.
613

614 Finzi AC, Norby RJ, Calfapietra C, Gallet-Budynek A, Gielen B, Holmes WE, Hoosbeek MR, Iversen CM,
615 Jackson RB, Kubiske ME, Ledford J, Liberloo M, Oren R, Polle A, Pritchard S, Zak DR, Schlesinger WH,
616 Ceulemans R. 2007. Increases in nitrogen uptake rather than nitrogen-use efficiency support higher rates
617 of temperate forest productivity under elevated CO₂. *Proceedings of the National Academy of Sciences*
618 104: 14014-14019.
619



- 620 Fleischer, K., Rammig, A., De Kauwe, M. G., Walker, A. P., Domingues, T. F., Fuchslueger, L., et al. (2019).
621 Amazon forest response to CO₂ fertilization dependent on plant phosphorus acquisition. *Nature*
622 *Geoscience*, 12(9), 736–741. <https://doi.org/10.1038/s41561-019-0404-9>
623
- 624 Fowler D, Steadman CE, Stevenson D, Coyle M, Rees RM, Skiba UM, Sutton MA, Cape JN, Dore AJ, Vieno
625 M, Simpson D, et al. Effects of global change during the 21st century on the nitrogen cycle. *Atmospheric*
626 *Chemistry and Physics*. 2015; 15(24): 13849-13893. <https://doi.org/10.5194/acp-15-13849-2015>
627
- 628 Franklin, O., Harrison, S.P., Dewar, R. *et al.* Organizing principles for vegetation dynamics. *Nat. Plants* 6,
629 444–453 (2020). <https://doi.org/10.1038/s41477-020-0655-x>
630
- 631 Gundersen, P., Emmett, B.A., Kjonaas, O.J., Koopmans, C.J. & Tietema, A. (1998) Impact of nitrogen
632 deposition on nitrogen cycling in forests: a synthesis of NITREX data. *Forest Ecology and Management*,
633 101, 37– 55.
634
- 635 Gurmessa, G.A., Wang, A., Li, S. *et al.* Retention of deposited ammonium and nitrate and its impact on the
636 global forest carbon sink. *Nat Commun* 13, 880 (2022). <https://doi.org/10.1038/s41467-022-28345-1>
637
- 638 Hijmans R (2023). *_raster: Geographic Data Analysis and Modeling_*. R package version 3.6-20,
639 <https://CRAN.R-project.org/package=raster>
640
- 641 Hungate, B.A., *et al.*, Nitrogen and Climate Change. *Science* 302, 1512-1513 (2003).
642 DOI:10.1126/science.1091390
643
- 644 Iversen C M, Bridgham S D and Kellogg L E 2010 Scaling plant nitrogen use and uptake efficiencies in
645 response to nutrient addition in peatlands *Ecology* 91 693–707
646
- 647 Jackman, S (2020). *pscl: Classes and Methods for R Developed in the Political Science Computational*
648 *Laboratory*. United States Studies Centre, University of Sydney. Sydney, New South Wales, Australia. R
649 package version 1.5.5.1. URL <https://github.com/atahk/pscl/>
650
- 651 Kanakidou, M., Myriokefalitakis, S., Daskalakis, N., Fanourgakis, G., Nenes, A., Baker, A. R., Tsigaridis, K.,
652 & Mihalopoulos, N. (2016). Past, present, and future atmospheric nitrogen deposition. *Journal of the*
653 *Atmospheric Sciences*, 73(5), 2039–2047. <https://doi.org/10.1175/JAS-D-15-0278.1>
654
- 655 Kuzyakov, Y. and Xu, X. (2013), Competition between roots and microorganisms for nitrogen: mechanisms
656 and ecological relevance. *New Phytol*, 198: 656-669. <https://doi.org/10.1111/nph.12235>
657
- 658 Le Quéré, C. et al., Global Carbon Budget 2018, *Earth Syst. Sci. Data*, 10, 2141-2194, DOI: 10.5194/essd-
659 10-2141-2018, 2018.
660
- 661 McIntire E, Chubaty A (2023). *_SpaDES.tools: Additional Tools for Developing Spatially Explicit Discrete*
662 *Event Simulation (SpaDES) Models_*. R package version 2.0.0, <[https://CRAN.R-](https://CRAN.R-project.org/package=SpaDES.tools)
663 [project.org/package=SpaDES.tools](https://CRAN.R-project.org/package=SpaDES.tools)>.
664
- 665 Niu, S., Classen, A.T., Dukes, J.S., Kardol, P., Liu, L., Luo, Y., Rustad, L., Sun, J., Tang, J., Templer, P.H.,
666 Thomas, R.Q., Tian, D., Vicca, S., Wang, Y.-P., Xia, J. and Zaehle, S. (2016), Global patterns and substrate-
667 based mechanisms of the terrestrial nitrogen cycle. *Ecol Lett*, 19: 697-
668 709. <https://doi.org/10.1111/ele.12591>
669
- 670 Peng, Y, Chen, HYH, Yang, Y. Global pattern and drivers of nitrogen saturation threshold of grassland
671 productivity. *Funct Ecol*. 2020; 34: 1979–1990. <https://doi.org/10.1111/1365-2435.13622>
672



- 673 Peng, Y., Prentice, I. C., Bloomfield, K. J., Campioli, M., Guo, Z., Sun, Y., Tian, Di, Wang, X., Vicca, S.,
674 & Stocker, B. D. (2023). Global terrestrial nitrogen uptake and nitrogen use efficiency. *Journal of*
675 *Ecology*, 111, 2676–2693. <https://doi.org/10.1111/1365-2745.14208>
676
- 677 Penuelas, J, Janssens, IA, Ciais, P, Obersteiner, M, Sardans, J. Anthropogenic global shifts in biospheric N
678 and P concentrations and ratios and their impacts on biodiversity, ecosystem productivity, food security,
679 and human health. *Glob Change Biol.* 2020; 26: 1962– 1985. <https://doi.org/10.1111/gcb.14981>
680
- 681 Poggio, L., de Sousa, L. M., Batjes, N. H., Heuvelink, G. B. M., Kempen, B., Ribeiro, E., and Rossiter, D.:
682 SoilGrids 2.0: producing soil information for the globe with quantified spatial uncertainty, *SOIL*, 7, 217–
683 240, <https://doi.org/10.5194/soil-7-217-2021>, 2021.
684
- 685 Prentice, I. C., Liang, X., Medlyn, B. E., & Wang, Y.-P. (2015). Reliable, robust and realistic: The three R's
686 of next-generation land-surface modelling. *Atmospheric Chemistry and Physics*, 15(10), 5987–6005.
687 <https://doi.org/10.5194/acp-15-5987-2015>
688
- 689 Ruehr, S., Keenan, T.F., Williams, C. et al. Evidence and attribution of the enhanced land carbon sink. *Nat*
690 *Rev Earth Environ* 4, 518–534 (2023). <https://doi.org/10.1038/s43017-023-00456-3>
691
- 692 Shcherbak I, Millar N and Robertson G P 2014 Global metaanalysis of the nonlinear response of soil nitrous
693 oxide (N₂O) emissions to fertilizer nitrogen *Proc. Natl Acad. Sci. USA* 111 9199–204
694
- 695 Sinsabaugh, R., Carreiro, M. & Repert, D. Allocation of extracellular enzymatic activity in relation to litter
696 composition, N deposition, and mass loss. *Biogeochemistry* 60, 1–24 (2002).
697 <https://doi.org/10.1023/A:1016541114786>
698
- 699 Sinsabaugh, R.L., Lauber, C.L., Weintraub, M.N., Ahmed, B., Allison, S.D., Crenshaw, C., Contosta, A.R.,
700 Cusack, D., Frey, S., Gallo, M.E., Gartner, T.B., Hobbie, S.E., Holland, K., Keeler, B.L., Powers, J.S., Stursova,
701 M., Takacs-Vesbach, C., Waldrop, M.P., Wallenstein, M.D., Zak, D.R. and Zeglin, L.H. (2008), Stoichiometry
702 of soil enzyme activity at global scale. *Ecology Letters*, 11: 1252-1264. [https://doi.org/10.1111/j.1461-](https://doi.org/10.1111/j.1461-0248.2008.01245.x)
703 0248.2008.01245.x
704
- 705 Sitch, S., Friedlingstein, P., Gruber, N., Jones, S. D., Murray-Tortarolo, G., Ahlström, A., et al. (2015). Recent
706 trends and drivers of regional sources and sinks of carbon dioxide. *Biogeosciences*, 12(3), 653–679.
707 <https://doi.org/10.5194/BG-12-653-2015>
708
- 709 Soudzilovskaia, N.A., Vaessen, S., Barcelo, M., He, J., Rahimlou, S., Abarenkov, K., Brundrett, M.C., Gomes,
710 S.I.F., Merckx, V. and Tedersoo, L. (2020), FungalRoot: global online database of plant mycorrhizal
711 associations. *New Phytol*, 227: 955-966. <https://doi.org/10.1111/nph.16569>
712
- 713 Stevens C J, Lind E M, Hautier Y and Harpole W S 2015 Anthropogenic nitrogen deposition predicts local
714 grassland primary production worldwide *Ecology* 96 1459–65
715
- 716 Stocker BD, Prentice IC, Cornell SE, Davies-Barnard T, Finzi AC, Franklin O, Janssens I, Larmola T, Manzoni
717 S, Näsholm T, Raven JA, et al. Terrestrial nitrogen cycling in Earth system models revisited. *New*
718 *Phytologist*. 2016; 210(4): 1165-1168. <https://doi.org/10.1111/nph.13997>
719
- 720 Sutton, M.A.; Fowler, D. 1993 Estimating the relative contribution of SO_x, NO_y and NH_x inputs to effects
721 of atmospheric deposition Critical loads: concept and applications. Grange-over-Sands Workshop
722
- 723 Terrer, C., Jackson, R. B., Prentice, I. C., Keenan, T. F., Kaiser, C., Vicca, S., et al. (2019). Nitrogen and
724 phosphorus constrain the CO₂ fertilization of global plant biomass. *Nature Climate Change*, 9(9), 684–
725 689. <https://doi.org/10.1038/s41558-019-0545-2>



- 726
727 Tian, D., Wang H., Sun, J., and Niu, S. Global evidence on nitrogen saturation of terrestrial ecosystem net
728 primary productivity. 2016. *Environmental Research Letters*, Volume 11, Number 2
729
730 Tian, D., Kattge, J., Chen, Y., Han, W., Luo, Y., He, J., Hu, H., Tang, Z., Ma, S., Yan, Z., Lin, Q., Schmid, B.,
731 Fang, J. 2019. A global database of paired leaf nitrogen and phosphorus concentrations of terrestrial
732 plants. *Ecology* 100(9): e02812.
733
734 Vallicrosa, H., J. Sardans, J. Maspons, and J. Peñuelas. 2022. "Global distribution and drivers of forest
735 biome foliar nitrogen to phosphorus ratios (N:P)." *Global Ecology and Biogeography* 31: 861–71.
736
737 Vallicrosa Pou, H. (2024). Global plant nitrogen uptake and nitrogen use efficiency. Zenodo.
738 <https://doi.org/10.5281/zenodo.13332734>
739
740 Vicca, S., Stocker, B. D., Reed, S., Wieder, W. R., Bahn, M., Fay, P. A., Janssens, I. A., Lambers, H., Peñuelas,
741 J., Piao, S., Rebel, K. T., Sardans, J., Sigurdsson, B. D., Sundert, K. V., Wang, Y. P., Zaehle, S., and Ciais, P.:
742 Using research networks to create the comprehensive datasets needed to assess nutrient availability as
743 a key determinant of terrestrial carbon cycling, *Environ. Res. Lett.*, 13,
744 125006, <https://doi.org/10.1088/1748-9326/aaeae7>, 2018.
745
746 Walker, T. W., and J. K. Syers. 1976. "Fate of Phosphorus during Pedogenesis." *Geoderma* 15: 1–19.
747 Soudzilovskaia, N.A., van Bodegom, P.M., Terrer, C. *et al.* Global mycorrhizal plant distribution linked to
748 terrestrial carbon stocks. *Nat Commun* 10, 5077 (2019). <https://doi.org/10.1038/s41467-019-13019-2>
749
750 Walker, A.P., De Kauwe, M.G., Bastos, A., Belmecheri, S., Georgiou, K., Keeling, R.F., McMahon, S.M.,
751 Medlyn, B.E., Moore, D.J.P., Norby, R.J., Zaehle, S., Anderson-Teixeira, K.J., Battipaglia, G., Brienen, R.J.W.,
752 Cabugao, K.G., Cailleret, M., Campbell, E., Canadell, J.G., Ciais, P., Craig, M.E., Ellsworth, D.S., Farquhar,
753 G.D., Fatichi, S., Fisher, J.B., Frank, D.C., Graven, H., Gu, L., Haverd, V., Heilman, K., Heimann, M., Hungate,
754 B.A., Iversen, C.M., Joos, F., Jiang, M., Keenan, T.F., Knauer, J., Körner, C., Leshyk, V.O., Leuzinger, S., Liu,
755 Y., MacBean, N., Malhi, Y., McVicar, T.R., Penuelas, J., Pongratz, J., Powell, A.S., Riutta, T., Sabot, M.E.B.,
756 Schleucher, J., Sitch, S., Smith, W.K., Sulman, B., Taylor, B., Terrer, C., Torn, M.S., Treseder, K.K., Trugman,
757 A.T., Trumbore, S.E., van Mantgem, P.J., Voelker, S.L., Whelan, M.E. and Zuidema, P.A. (2021), Integrating
758 the evidence for a terrestrial carbon sink caused by increasing atmospheric CO₂. *New Phytol*, 229: 2413-
759 2445. <https://doi.org/10.1111/nph.16866>
760
761 Wang R, Goll D, Balkanski Y, Hauglustaine D, Boucher O, Ciais P, Janssens I, Peñuelas J, Guenet B, Sardans
762 J et al. 2017. Global forest carbon uptake due to nitrogen and phosphorus deposition from 1850–2100.
763 *Global Change Biology* 23: 4854–4872.
764
765 Wang, X., Zhao, X. (Eds.), 2022. Protocol for Field Investigation and Literature Data Compilation of Carbon
766 Storage in Terrestrial Ecosystems. Science Press, Beijing.
767
768 Wickham, H. *ggplot2: Elegant Graphics for Data Analysis*. Springer-Verlag New York, 2016.
769
770 Wickham H, Henry L (2023). *_purrr: Functional Programming Tools_*. R package version 1.0.2,
771 <<https://CRAN.R-project.org/package=purrr>>.
772
773 WU, Z., DIJKSTRA, P., KOCH, G.W., PEÑUELAS, J. and HUNGATE, B.A. (2011), Responses of terrestrial
774 ecosystems to temperature and precipitation change: a meta-analysis of experimental manipulation.
775 *Global Change Biology*, 17: 927-942. <https://doi.org/10.1111/j.1365-2486.2010.02302.x>
776



- 777 Xu, X., Thornton, P.E. and Post, W.M. (2013), Global soil microbial biomass C, N and P. *Global Ecology and*
778 *Biogeography*, 22: 737-749. <https://doi.org/10.1111/geb.12029>
779
- 780 Yang, J. and Tian, H. (2022): ISIMIP3a N-deposition input data (v1.2). ISIMIP Repository.
781 <https://doi.org/10.48364/ISIMIP.759077.2>
782
- 783 Zaehle S, Medlyn BE, De Kauwe MG, Walker AP, Dietze MC, Hickler T, Luo Y, Wang YP, El-Masri B, Thornton
784 P, Jain A, et al. Evaluation of 11 terrestrial carbon-nitrogen cycle models against observations from two
785 temperate Free-Air CO₂ Enrichment studies. *New Phytologist*. 2014; 202(3): 803-822.
786 <https://doi.org/10.1111/nph.12697>
787
- 788 Zhou G, Terrer C, Huang A, Hungate BA, van Gestel N, Zhou X, van Groenigen KJ. Nitrogen and water
789 availability control plant carbon storage with warming. *Sci Total Environ*. 2022 Dec 10;851(Pt 1):158243.
790 doi: 10.1016/j.scitotenv.2022.158243. Epub 2022 Aug 23. PMID: 36007637.